Age-related normative changes in cerebral perfusion: Data from The Irish Longitudinal Study on Ageing (TILDA)

Caoilfhionn Ní Leidhin [a,b], Jason McMorrow [a,b], Daniel Carey [a,c], Louise Newman [a,c], Wilby Williamson [a,d], Andrew J. Fagan [e], Michael A. Chappell [f,g,h,i], Rose Anne Kenny [a,c,d,j], James F. Meaney [a,b], Silvin P. Knight [a,c,*]

[a] School of Medicine, Trinity College Dublin, Ireland
[b] The National Centre for Advanced Medical Imaging (CAMI), St. James's Hospital, Dublin, Ireland
[c] The Irish Longitudinal Study on Ageing (TILDA), Trinity College Dublin, Ireland
[d] The Global Brain Health Institute (GBHI), Trinity College Dublin, Ireland
[e] Department of Radiology, Mayo Clinic, Rochester, MN, USA
[f] Radiological Sciences, Division of Clinical Neuroscience, School of Medicine, University of Nottingham, Nottingham, United Kingdom
[g] Sir Peter Mansfield Imaging Center, School of Medicine, University of Nottingham, Nottingham, United Kingdom
[h] Nottingham Biomedical Research Centre, Queens Medical Centre, University of Nottingham, Nottingham, United Kingdom
[i] Wellcome Centre for Integrative Neuroimaging, Nuffield Department of Clinical Neurosciences, University of Oxford, Oxford, United Kingdom
[j] Mercer's Institute for Successful Ageing, St. James's Hospital, Dublin, Ireland

ARTICLE INFO

ABSTRACT

Objective: To establish normative reference values for total grey matter cerebral blood flow (CBF_{GM}) measured using pseudo-continuous arterial spin labelling (pCASL) MRI in a large cohort of community-dwelling adults aged 54 years and older.

Background: Quantitative assessment of CBF_{GM} may provide an imaging biomarker for the early detection of those at risk of neurodegenerative diseases, such as Alzheimer's and dementia. However, the use of this method to differentiate normal age-related decline in CBF_{GM} from pathological reduction has been hampered by the lack of reference values for cerebral perfusion.

Methods: The study cohort comprised a subset of wave 3 (2014–2015) participants from The Irish Longitudinal Study on Ageing (TILDA), a large-scale prospective cohort study of individuals aged 50 and over. Of 4309 participants attending for health centre assessment, 578 individuals returned for 3T multi-parametric MRI brain examinations. In total, CBF_{GM} data acquired from 468 subjects using pCASL-MRI were included in this analysis. Normative values were estimated using Generalised Additive Models for Location Shape and Scale (GAMLSS) and are presented as percentiles, means and standard deviations.

Results: The mean age of the cohort was 68.2 ± 6.9 years and 51.7% were female. Mean CBF_{GM} for the cohort was 36.5 ± 8.2 ml/100 g/min. CBF_{GM} decreased by 0.2 ml/100 g/min for each year increase in age (95% CI = −0.3, −0.1; $p \leq 0.001$) and was 3.1 ml/100 g/min higher in females (95% CI = 1.6, 4.5; $p \leq 0.001$).

Conclusions: This study is by far the largest single-site study focused on an elderly community-dwelling cohort to present normative reference values for CBF_{GM} measured at 3T using pCASL-MRI. Significant age- and sex-related differences exist in CBF_{GM}.

1. Introduction

The world population aged 60 years and older is predicted to increase from 900 million to 2.1 billion between 2015 and 2050, with an anticipated 350% increase in individuals aged 80 years or older (United Nations, 2015). Ageing is associated with increased morbidity from multiple causes, including dementia, the incidence of which is predicted to triple from 47 million currently to 140 million by 2050 (World Health Organization, 2015). These demographic changes will impose profound socioeconomic stresses on healthcare systems.

Vascular disease is an important contributor to brain ageing and dementia. Due to the brain's high metabolic rate and limited capacity

for substrate storage, strict control of cerebral blood flow (CBF) via metabolic, autonomic and cerebral autoregulation is critical to ensure adequate oxygen and nutrient supply to the brain (Willie et al., 2014). Cerebral hypoperfusion has been suggested as a potential link between vascular damage and dementia, with prior studies having reported lower cerebral perfusion in patients with mild cognitive impairment and dementia (Leijenaar et al., 2017; Luckhaus et al., 2008; Wolters et al., 2017). Additionally, a reduction in CBF in high-risk subjects for Alzheimer's disease has been reported to occur *before* the onset of cognitive decline, brain atrophy or amyloid-β accumulation (Zhang et al., 2017), suggesting that cerebral hypoperfusion may act as a biomarker heralding Alzheimer's disease. Once detected, it could potentially offer a target for intervention. However, since ageing itself is associated with impaired regulatory mechanisms and therefore lower CBF, a significant challenge for researchers and clinicians is to distinguish normal age-related decline in cerebral perfusion from pathological reduction.

Accurate measurement of cerebral perfusion has proved challenging, with most techniques being costly, invasive, relying on exposure to ionising radiation and/or subject to operator variability. Arterial spin labelling (ASL) is an MRI technique that uses inflowing magnetically-labelled arterial blood as an endogenous tracer to measure cerebral haemodynamics and provides a quantitative, non-invasive, non-ionising measure of CBF. This method is gaining acceptance as an optimal technique for population-based CBF assessment (Wintermark et al., 2005), with high concordance rates reported between ASL-MRI and [^{15}O]-water positron emission tomography (PET); currently considered the 'gold standard' for measuring whole brain perfusion (Fan et al., 2016).

Given the lack of reference values for cerebral perfusion measured using ASL-MRI, this study was performed to establish normative values for CBF in a large cohort of community-dwelling adults aged 54 years and older.

2. Materials and methods

2.1. Subject cohort – The Irish Longitudinal Study on Ageing (TILDA)

This research was carried out on a subset of participants enrolled in The Irish Longitudinal Study on Ageing (TILDA), which is described in detail in previous publications (Kearney et al., 2011; Whelan and Savva, 2013). In brief, TILDA is a prospective, cohort study, which collects health, economic and social data from nationally-representative, community-dwelling Irish adults and investigates how various factors interact. 8507 adults were enrolled in the first wave of TILDA (2009–2010).

The cohort used in the present study was comprised of a subset of TILDA wave 3 (2014–2015) participants. Of 4309 participants attending for health assessment in a dedicated health assessment centre, a random subset was invited to return for multi-parametric brain MRI at the National Centre for Advanced Medical Imaging (CAMI), Dublin, Ireland. Participants were excluded if they had a contraindication to MRI or a prior stroke/head injury. MRIs were performed between May 2014 and June 2015. A total of 560 scans were obtained from 578 subjects attending for MRI (Donoghue et al., 2018). T_1-weighted and ASL data were available for 546 participants (attrition due to claustrophobia or inability to complete scan - pCASL data was acquired last in the examination sequence).

A trained operator (DC) who was blind to participant identity screened all T_1-weighted imaging for image artefacts and/or pathology. 22 subjects were excluded due to abnormalities on T_1-weighted imaging. Among those, sixteen had gross abnormality corresponding to confluent white matter hyperintensities on T_2 and FLAIR imaging, four had established large vessel infarcts and two had MRI evidence of prior contusion/haemorrhage. One patient with Parkinson's disease, four with a history of stroke and four with a Mini Mental State Examination (MMSE) score <24 were also excluded from data analysis. Another trained oper-

ator (CNL) who was blind to participant identity reviewed all perfusion maps for evidence of arterial artefact, poor labelling of a feeding artery, severe motion and/or other gross failure to produce a perfusion image (see Appendix 1 for further details). By consensus between CNL and MC, 29 subjects with abnormal perfusion maps were removed from the cohort. Of those, 18 were excluded due to labelling failure, 4 due to delayed arrival and 7 due to severe motion (see Appendix 1 for examples). An additional three subjects were removed as outliers due to extreme whole brain CBF_{GM} values (< 10 (n=1) or >100ml/100g/min. (n=2)). Additionally, 15 were excluded due to extremes of age. The small numbers of participants aged younger than 54 and older than 84 would result in unreliable normative value estimates. This left a total of 468 subjects for whom CBF data were available. Exclusionary criteria leading to the final sample are illustrated in the Fig. 1.

2.2. TILDA health assessment

The comprehensive TILDA health assessment has been described in detail elsewhere (Cronin et al., 2013; Kenny et al., 2013). Socio-demographic, behavioural and physical health characteristics of participants were recorded. These included age, sex, self-reported alcohol consumption, smoking status and cardiovascular conditions. Use of antihypertensive medication(s) was documented. Physical measures including height and weight (thereby allowing calculation of body mass index [BMI]), blood pressure (static seated and standing, as well as dynamic beat-to-beat variability) and pulse wave velocity were also recorded. Participants were screened for depression and cognitive impairment/dementia using the Center for Epidemiologic Studies Depression scale (CESD) and Mini-Mental State Examination (MMSE) respectively.

2.3. MRI data acquisition

All MRI examinations were performed on a 3T system (*Achieva*, Philips Medical Systems, The Netherlands), using a 32-channel head coil. The MRI protocol included T_1-weighted and ASL sequences. T_1-weighted 3D magnetization-prepared rapid gradient echo (MPRAGE) anatomical images were acquired over 5 min 24 s with the following scan parameters: field of view (FOV) = 240 × 240 × 162 mm^3, matrix = 288 × 288 × 180, repetition time (TR) = 6.7 ms, echo time (TE) = 3.1 ms, flip angle = 8°, and SENSE = 2. The specific ASL implementation used in this study was pseudo-continuous ASL (pCASL). This involves the application of a closely spaced train of inversion pulses to label upstreaming arterial blood in the neck, followed by a delay to allow the labelled blood to perfuse the brain tissue and finally, imaging of the perfused brain. Imaging was achieved via 2D multislice single shot echo-planar imaging (EPI). The distance between the centre of the imaged volume and the centre of the labelling slice was 90 mm. Positioning the labelling plane 32 mm below the base of the imaging volume ensured that the feeding (carotid) arteries were consistently perpendicular to the labelling plane and below the inferior border of the cerebellum. This prescription further ensured the labelling plane was remote from regions of strong susceptibility artefacts such as air/tissue interfaces. Background tissue suppression was performed twice during the pCASL sequence. First, prior to the labelling block, pre-saturation of the tissue within the imaged volume was performed using WET (water suppression enhanced through T_1 effects) (Ogg et al., 1994). Second, two 180° inversion pulses were applied between the labelling and image acquisition blocks. The first inversion pulse was selective to the imaged volume and was applied 60 ms after the end of the labelling pulse, while the second was non-selective and was applied 1,080 ms after the end of the labelling pulse. Two inversion pulses were found to represent a good trade-off between background tissue suppression and ASL signal. pCASL acquisition parameters were as follows: FOV = 240 × 240 mm^2, matrix = 80 × 80, TR = 4000 ms, TE = 9 ms, FA = 90°, SENSE = 2.5, and scan duration = 4 min 16 s. 13 slices (8 mm thick, 1 mm gap) were
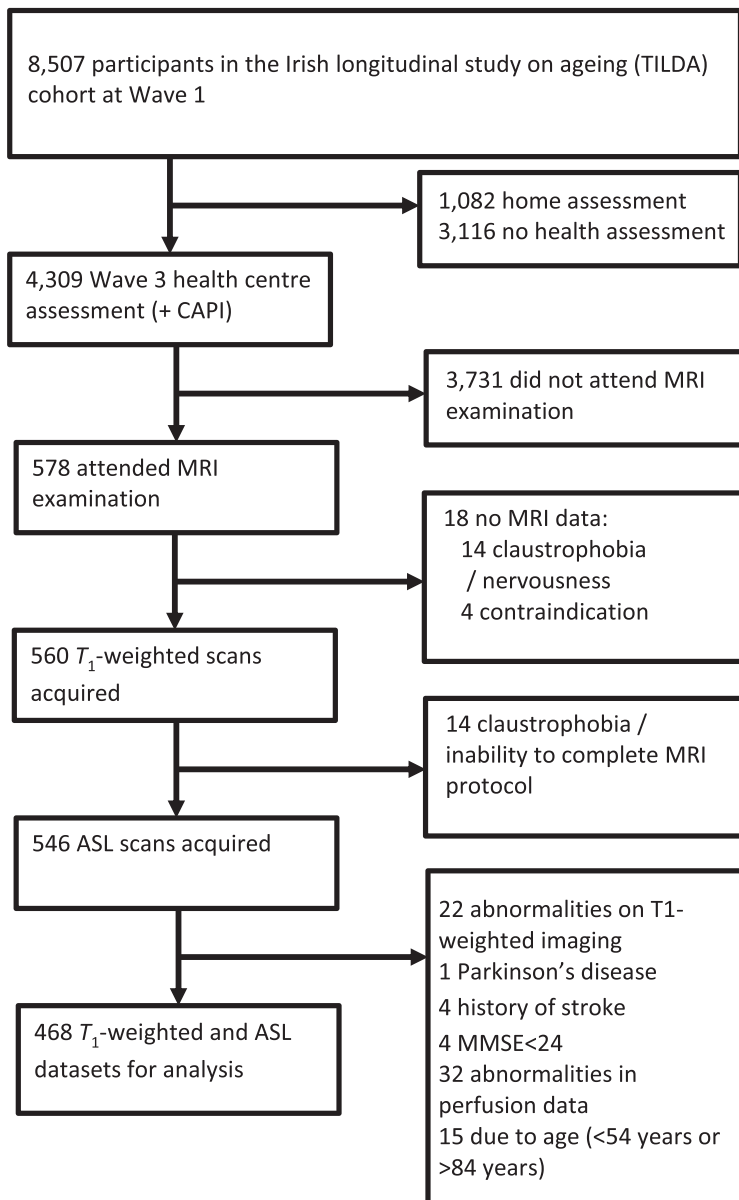
```
8,507 participants in the Irish longitudinal study on ageing (TILDA)
cohort at Wave 1
        │
        │────────────────→  1,082 home assessment
        │                   3,116 no health assessment
        ▼
4,309 Wave 3 health centre
assessment (+ CAPI)
        │
        │────────────────→  3,731 did not attend MRI
        │                   examination
        ▼
578 attended MRI
examination
        │
        │────────────────→  18 no MRI data:
        │                      14 claustrophobia
        │                       / nervousness
        │                      4 contraindication
        ▼
560 T₁-weighted scans
acquired
        │
        │────────────────→  14 claustrophobia /
        │                   inability to complete MRI
        │                   protocol
        ▼
546 ASL scans acquired
        │
        │────────────────→  22 abnormalities on T1-
        │                   weighted imaging
        │                   1 Parkinson's disease
        │                   4 history of stroke
        │                   4 MMSE<24
        │                   32 abnormalities in
        │                   perfusion data
        │                   15 due to age (<54 years or
        │                   >84 years)
        ▼
468 T₁-weighted and ASL
datasets for analysis
```

acquired sequentially in a caudocranial direction, yielding 30 dynamic scans and 780 images in total (390 labelled, 390 unlabelled). An imaging volume of 116 mm was considered a compromise between covering as much of the brain as possible and limiting MRI acquisition time, in this older cohort. A labelling duration of 1800 ms and a post-label delay (PLD) of 1800 ms were used, as recommended in the ASL consensus paper (Alsop et al., 2015). Given the broad age range among the study cohort (53–84, mean 68.5 years) and the desire to use a consistent acquisition protocol, a PLD of 1800 ms was employed. This took into account the 2D multi-slice readout and consequent prolonged PLDs in more superior slices. This PLD would ideally minimize large vessel arterial inflow signal in the pCASL images, while maximizing signal-to-noise ratio (Haller et al., 2016) in this older cohort with presumed longer arterial arrival times.

Calibration scans measuring the equilibrium magnetisation (M_0) were also acquired using the same geometry as the pCASL sequence, with TR = 10,000 ms, TE = 9 ms, and scan duration = 20 s. B_0 field maps were measured using a two-echo 2D gradient echo sequence with the same in-plane resolution as the pCASL scans and the following acquisition parameters: 38 slices (3.2 mm slice thickness, 0.3 mm slice gap), TR = 455 ms, TE_1 / TE_2 = 1.69 / 7.0 ms, FA = 90°, and scan duration = 39 s.

2.4. MRI analysis

MRI analysis was performed using *Oxford_ASL v4.0* in *FMRIB Software Library (BASIL - FSL;* Oxford Centre for Functional MRI of the Brain, Oxford, UK, HYPERLINK " https://fsl.fmrib.ox.ac.uk/fsl/fslwiki/BASIL) (Chappell et al., 2009; Groves et al., 2009; Woolrich et al., 2009). Quantification in BASIL used the standard well-mixed single compartment kinetic model with no dispersion of the bolus of labelled blood water (Buxton, 2005). A tissue T_1 value of 1300 ms and an arterial blood T_1 of 1,650 ms were assumed, along with a blood-brain partition coefficient of 0.9. The labelling efficiency was set at 0.85 (Alsop et al., 2015). Slice-timing effects, which increase the PLD for more superior slices, were corrected for a slice delay of 30 ms. Motion correction was performed on the raw ASL data within BASIL using FSL MCFLIRT. Adaptive spatial regularisation was used to decrease the appearance of noise in the final perfusion image (Groves et al., 2009). Perfusion images were reviewed for evidence of image artefacts, as described previously. Anatomical processing was performed using the *fsl_anat* function, including segmentation and registration to MNI152 standard space. BASIL performed linear registration of the perfusion image to the anatomical image. B_0 maps were used to apply distortion corrections to the pCASL images in order

to compensate for any spatially nonlinear image distortion effects that B_0 inhomogeneities may have had on these EPI data.

Voxel-wise absolute perfusion values (CBF in ml/100g/min) were calculated using the calibration (M_0) data (Alsop et al., 2015). M_0 values for arterial blood were estimated indirectly using cerebrospinal fluid (CSF) as a 'reference-tissue' (measured in the ventricles using an automatically generated mask in BASIL that is based on a combination of the CSF segmentation from fsl_anat and the ventricular regions of interest in the Harvard-Oxford Atlas). A correction was made for incomplete recovery of the signal based on the TR and an assumed T_1 value for CSF (4300 ms), as well as the differences in T_2 values between tissue (150 ms) and CSF (750 ms). Mean whole brain grey matter cerebral blood flow (CBF_{GM}) was calculated in the native space of the perfusion image. In order to create a grey matter mask, the grey matter partial volume estimates from the structural segmentation were transformed into pCASL space and a threshold of 70% grey matter applied (Chappell et al., 2017). A reasonably conservative threshold of 70% grey matter was chosen to reduce the partial volume effect on mean GM values.

2.5. Statistical analysis

Generalised Additive Models for Location, Shape and Scale (GAMLSS), calculated in statistical software *R* (version 3.4.3, MA, USA) were used to estimate normative reference values for CBF_{GM}. CBF_{GM} was modelled using the Box-Cox Power Exponential distribution, which has four parameters corresponding to location, scale, skew and kurtosis of the distribution (Rigby and Stasinopoulos, 2005; Rigby and Stasinopoulos, 2004). Age was included as a continuous variable in the models, with sex as a covariate. Interactions between age and sex were also considered. Restricted cubic splines were used in the models to account for the potentially non-linear relationship between CBF and age. Model selection utilised a forward and backward stepwise selection criteria based on the Akaike Information Criterion. CBF_{GM} is reported for the 5th, 10th, 25th, 50th, 75th, 90th and 95th percentiles for each sex for every fifth year of age from 54 and 84. Statistical analysis also included linear regressions performed in *STATA* (12.1, StataCorp, TX, USA). Statistical significance was set at $p < 0.05$.

3. Results

3.1. Subject characteristics

Mean (SD) age at the time of scanning was 68.4 (7.2) years for males and 68.0 (6.7) years for females. 51.7% of participants were female Table 1.

3.2. Cerebral perfusion values

Mean CBF_{GM} was 36.5 ± 8.2 ml/100 g/min; range: [12.9–66.4 ml/100 g/min]. CBF_{GM} decreased by 0.2 ml/100 g/min with every one year increase in age (95% CI = −0.3, −0.1, $p \leq 0.001$; model adjusted for sex) and was 3.1 ml/100 g/min higher in females (95% CI = 1.6, 4.5, $p \leq 0.001$; model adjusted for age) Figure 2.

Normative reference values for CBF_{GM} are presented in Table 3 and illustrated in Fig. 3, stratified by age and sex according to percentiles. In men, average CBF_{GM} decreased by 15.2% across the age range tested from 37.6 ml/100 g/min (interquartile range [IQR]: 32.1–42.1 ml/100 g/min) in the youngest (54 years) to 31.9 ml/100g/min (IQR: 27.3–35.8 ml/100 g/min) in the oldest (84 years). A similar trend was observed in women, with average CBF_{GM} decreasing 13.7 % from 41.0 ml/100 g/min (IQR: 35.1–46.0 ml/100 g/min) to 35.4 ml/100 g/min (IQR: 30.3–39.7 ml/100 g/min) across the same age range. Reference curves (Fig. 3) demonstrate linear CBF_{GM} decline with age.

Table 1
Characteristics of study sample.

	Study Cohort (N = 468)
Age [years]	
Male	68.4 (SD: 7.2, range: [53–84])
Female	68.0 (SD: 6.7, range: [53–84])
Sex [% (n)]	Female: 51.7% (242)
Education [% (n)]	
Primary/None	19.7% (92)
Secondary	36.3% (170)
Third/Higher	44.0% (206)
Mean BMI [kg/m²]	27.8 (SD: 4.3, range: [17.9–45.8])
Self-reported diabetic [% (n)]	
Yes	7.9% (37)
Number of Cardiovascular Conditions [a] [% (n)]	
0	38.5% (180)
1	35.9% (168)
2+	25.6% (120)
High Blood Pressure [% (n)]	
Yes	34.2% (160)
High Cholesterol [% (n)]	
Yes	36.1% (169)
Mean Systolic BP [mmHg]	134.4 (SD: 19.3, range: [87.0–212])
Mean Diastolic BP [mmHg]	80.1 (SD: 10.5, range: [51.5–118])
Mean MAP [mmHg]	98.2 (SD: 12.5, range: [64.5–144])
Mean PWV [m/s]	10.8 (SD: 2.0, range: [5.8–18.6])
Antihypertensive Medication Use [b] [% (n)]	
Yes	39.5% (185)
CAGE Alcohol Scale [% (n)]	
CAGE < 2	80.1% (375)
CAGE ≥ 2	9.0% (42)
No response	10.9% (51)
Smoker [% (n)]	
Never	50.9% (238)
Past	42.5% (199)
Current	6.6% (31)
CESD [% (n)]	
Non-depressed (CESD <9)	90.6% (424)
Depressed (CESD ≥9)	9.4% (44)
Mean MMSE	28.9 (SD: 1.3, range: [24–30])
Mean CBF_{GM} [ml/100g/min]	36.5 (SD: 8.2, range: [12.9–66.4])

[a] Cardiovascular conditions: high cholesterol; high blood pressure; angina; heart attack ever; heart failure, murmur, abnormal rhythm; stroke ever, TIA ever.

[b] Coded using the Anatomical Therapeutic Chemical Classification (ATC): antihypertensive medications (ATC C02), diuretics (ATC C03), β-blockers (ATC C07), calcium channel blockers (ATC C08), and renin-angiotensin system agents (ATC C09) Abbreviations: BMI, body mass index; PWV, pulse wave velocity; BP, blood pressure; MAP, mean arterial pressure; CESD, Center for Epidemiologic Studies Depression scale; MMSE, Mini-Mental State Examination; CBF_{GM}, grey matter cerebral blood flow.

3.3. Cardiovascular determinants of cerebral perfusion

CBF_{GM} decreased by 0.06, 0.14, and 0.11 ml/100 g/min per 1 mmHg increase in systolic blood pressure (BP) ($p \leq 0.001$, 95% CI = −0.10, −0.03), diastolic BP ($p \leq 0.001$, 95% CI = −0.20, −0.07) mean arterial pressure (MAP) ($p \leq 0.001$, 95% CI = −0.17, −0.06) respectively, all models adjusted for age and sex. CBF_{GM} decreased by 0.35 ml/100 g/min for each 1 unit increase in body mass index ($p \leq 0.001$, 95% CI = −0.51, −0.18; model adjusted for age and sex). There was no significant association between grey matter perfusion and self-reported educational attainment, diabetes, number of cardiovascular conditions, high blood pressure, hypercholesterolaemia, antihypertensive medication(s), CAGE score>2, smoking, depression, or MMSE performance. For further details see Table 2.

4. Discussion

With increasing age, there is both a decline in CBF_{GM} and in the regulatory mechanisms that maintain adequate brain perfusion. To date, the lack of published CBF_{GM} normative values in large populations has
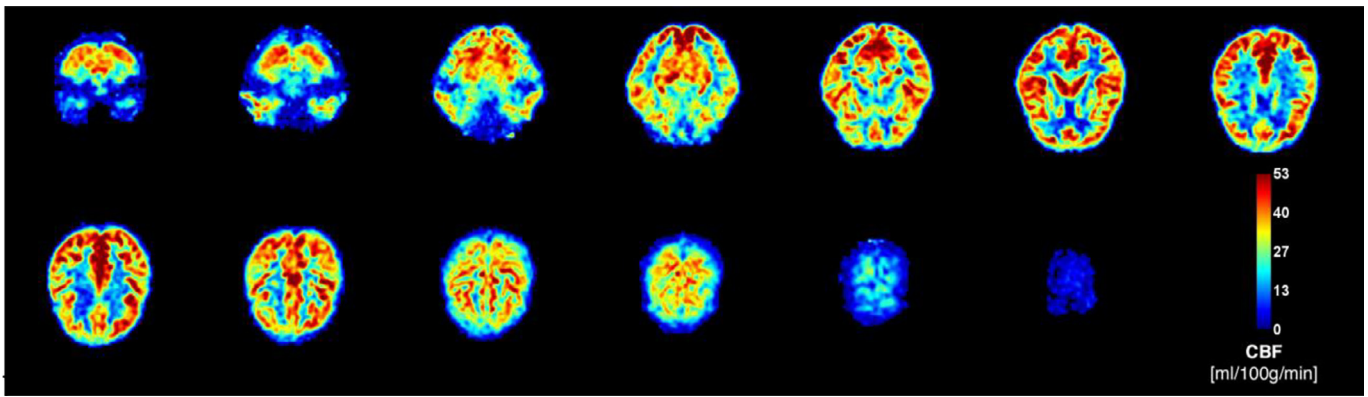
Fig. 2. Example of processed perfusion map measured with ASL from a 65-year-old female participant.
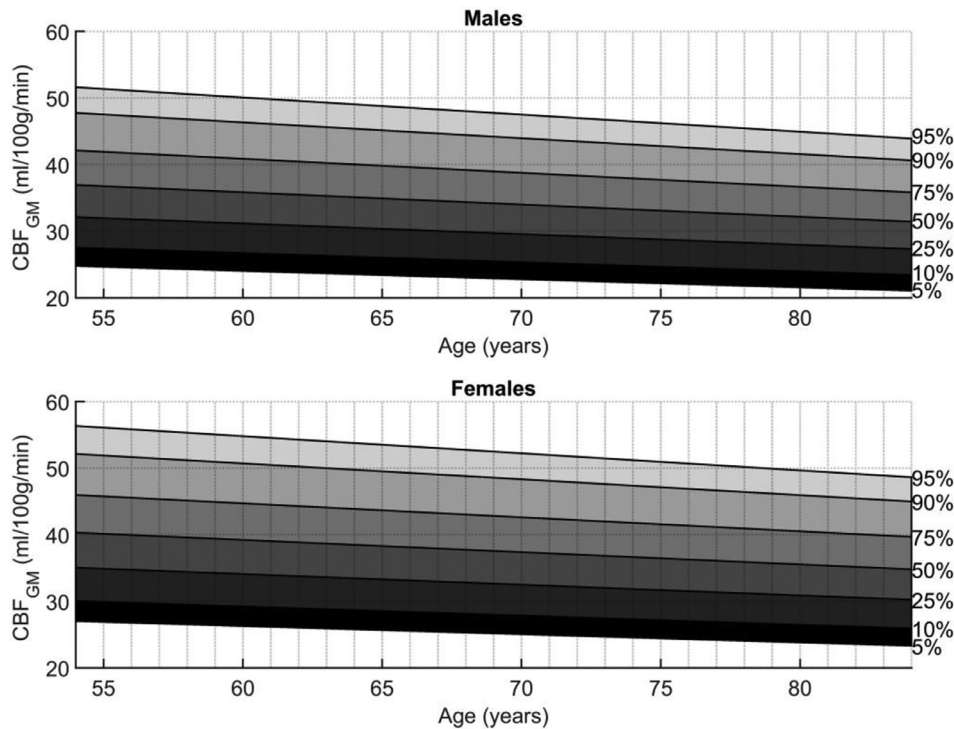

Fig. 3. Age-dependence of total grey matter cerebral blood flow (CBF$_{GM}$) stratified by sex, for men (top) and women (bottom). Figure displays normative values for grey matter CBF according to percentiles.

hindered acceptance of this potentially useful biomarker in distinguishing normal age-related decline in CBF$_{GM}$ from pathological reduction. In this study, normative CBF$_{GM}$ values measured using pCASL-MRI in 468 community-dwelling subjects are presented.

Consistent with prior studies using various imaging modalities(Chen et al., 2011; De Vis et al., 2015; Liu et al., 2012; Lu et al., 2011; Parkes et al., 2004; Selim et al., 2008; Soni et al., 2016; Vernooij et al., 2008; Wolters et al., 2017), this research demonstrates declining cerebral blood flow with advancing age. Reference curves demonstrate linear decline in CBF$_{GM}$ with age, with comparable overall CBF$_{GM}$ decrease with time in men and women.

Few studies to date have reported on CBF values in older adults and of those that have, a consensus on normative CBF values has not been reached. Direct comparison between the present study and previous ones is limited due to significant variations in study methodologies. However, the present study followed best-practice ISMRM consensus guidelines and results are in line with those where CBF was measured using 3T pCASL-MRI according to ISMRM recommendations. Following a similar protocol to ours, Jefferson *et al.* reported mean total whole brain CBF values of 37.3 ± 7.1 ml/100 g/min for 270 adults

with a mean age of 73 ± 7 years (Jefferson et al., 2018). Chen et al., in a smaller study using 3T pCASL MRI, reported higher mean cortical CBF$_{GM}$ values of 52.6 ± 9.3, 52 ± 10.7 and 42.7 ± 8.8 ml/100 g/min in younger (mean age 30 ± 6 years, $n = 11$), middle-aged (mean age 52 ± 6 years, n=38) and older adults (mean age 71 ± 10 years, n=37) respectively (Chen et al., 2011). The largest population-based MRI study to date using 2D phase-contrast MRI at 1.5T reported mean total cerebral perfusion of 56.3 ± 9.7 ml/100 g/min in 4759 subjects with a mean age of 64 ± 11 years (Wolters et al., 2017). pCASL-MRI has an advantage over phase-contrast (PC) MRI, in that it directly measures CBF at a voxel level as opposed to measuring blood flow velocities through the internal carotid and vertebral arteries, which can be used to calculate volumetric blood flow to the brain (Juttukonda and Donahue, 2019). Although CBF values measured with pCASL and PC MRI are similar, PC estimates tend to be higher and more variable (Dolui et al., 2016). In a study of 541 healthy middle-aged subjects comparing pCASL and PC MRI at 3T, Dolui et al. reported CBF values of 47.7 ± 9.8 ml/100 g/min with pCASL versus 55.8 ± 12.1 ml/100 g/min with PC MRI (Dolui et al., 2016).

Previous research has suggested that age-related decrease in cerebral perfusion is potentially a consequence of cerebral atrophy, and/or de-

Table 2

Age and sex (and education for MMSE) adjusted associations of demographic characteristics, cardiovascular risk factors and measures, medications and cognitive performance with grey matter cerebral blood flow (CBF$_{GM}$ [ml/100 g/min]).

	β (95% CI)	P Value
CBF$_{GM}$ [ml/100 g/min] (N = 468)		
Education [Ref: Primary/None]		
Secondary	0.17 (−1.89 to 2.24)	0.870
Third/Higher	−0.49 (−2.524 to 1.53)	0.631
BMI [per 1 kg/m^2]	−0.35 (−0.51 to −0.18)	≤0.001
Self-reported diabetic [Ref: No]		
Yes	−1.06 (−3.56 to 1.45)	0.408
Number of Cardiovascular Conditions[a] [Ref: 0]		
1	−0.09 (−1.70 to 1.53)	0.916
2+	−0.43 (−2.43 to 1.157)	0.673
High Blood Pressure [Ref: No]		
Yes	−0.95 (−2.51 to 0.6)	0.232
High Cholesterol [Ref: No]		
Yes	0.78 (−0.77 to 2.33)	0.323
PWV [per 1 m/s]	−0.11 (−0.51 to 0.29)	0.592
Systolic BP [per 1 mmHg]	−0.06 (−0.10 to −0.03)	≤0.001
Diastolic BP [per 1 mmHg]	−0.14 (−0.20 to −0.07)	≤0.001
MAP [per 1 mmHg]	−0.11 (−0.17 to −0.06)	≤0.001
Antihypertensive Medication Use [b] [Ref: No]		
Yes	−0.86 (−2.35 to 0.63)	0.258
CAGE Alcohol Scale [Ref: CAGE < 2]		
CAGE ≥ 2	−1.31 (−3.03 to 0.40)	0.133
No response	−1.43 (−3.87 to 1.02)	0.251
Smoker [Ref: Never]		
Past	−0.95 (−2.43 to 0.53)	0.207
Current	−0.27 (−3.46 to 2.92)	0.869
CESD [Ref: CESD <9]		
Depressed (CESD ≥9)	0.99 (−1.31 to 3.29)	0.397
	IRR (95% CI)	P Value
MMSE [per 1 error][c]	1.00 (0.98 to 1.01)	0.411

[a] Cardiovascular conditions: high cholesterol; angina; heart attack ever; heart failure, murmur, abnormal rhythm; stroke ever, TIA ever.

[b] Coded using the Anatomical Therapeutic Chemical Classification (ATC): antihypertensive medications (ATC C02), diuretics (ATC C03), β-blockers (ATC C07), calcium channel blockers (ATC C08), and renin-angiotensin system agents (ATC C09).

[c] Also adjusted for educational attainment. Abbreviations: CI, confidence intervals; BMI, body mass index; PWV, pulse wave velocity; BP, blood pressure; MAP, mean arterial pressure; CESD, Center for Epidemiologic Studies Depression scale; MMSE, Mini-Mental State Examination; IRR, incidence rate ratio; CBF$_{GM}$, grey matter cerebral blood flow.

creased neuronal/metabolic activity and demand (Parkes et al., 2004; Zhang et al., 2017). However, this is not universally accepted as other studies have found regional reductions in CBF (using pCASL and surface-based analyses to map cerebral perfusion and cortical thickness) to be independent of age-related atrophy (Chen et al., 2011). The Rotterdam study demonstrated the bidirectional nature of this relationship, reporting that smaller baseline brain volume results in steeper decrease in CBF over time. However, they also found that lower CBF at baseline is associated with accelerated brain atrophy, *only* in subjects aged 65 years or older (Zonneveld et al., 2015). This finding suggests that the relationship between CBF and atrophy is more complex in the older population.

Although this study assessed only CBF$_{GM}$ as a marker of global cerebral perfusion in older adults, prior studies have demonstrated regional age-related differences in CBF. Indeed, regions of both increased and decreased perfusion have been observed in cognitively normal older subjects. For example, blood flow to the parietal cortex and precuneus may be reduced, while other regions, including the temporal lobe, posterior and anterior cingulate cortex may demonstrate elevated CBF (Lee et al., 2009; Preibisch et al., 2011; Zhang et al., 2018). Prior ASL studies have demonstrated hypoperfusion of the posterior cingulate gyrus and precuneus in patients with mild cognitive impairment/Alzheimer's disease (Thomas et al., 2019). Thus regional hypoperfusion in older subjects may indicate vulnerability to cognitive impairment/Alzheimer's disease, whereas hyperperfusion may represent a compensatory response.

The results presented in this study corroborate higher cerebral perfusion in females compared to males, as reported previously (Jennings et al., 2013; Liu et al., 2012; Parkes et al., 2004; Selim et al., 2008; Soni et al., 2016; Wolters et al., 2017), with a 3.1 ml/100 g/min discrepancy. While this cross-sectional study does not allow for causal inference, previous research has suggested that this finding may reflect lower haematocrit and blood viscosity and higher cerebral metabolic rates for glucose and oxygen in women (Tarumi and Zhang, 2018).

Prior research indicates that obesity and hypertension can alter both the structure and function of cerebral arteries, thereby decreasing the compliance of the cerebrovasculature (Dorrance et al., 2014; Pires et al., 2013; Rogers et al., 1985). In addition, aortic stiffening caused by ageing and hypertension results in transmission of damaging high-pressure pulsatility to the cerebral microvasculature (de Roos et al., 2017). These processes can increase the risk of cerebral hypoperfusion. It is unsurprising, therefore, that our study, as with prior research, demonstrates a significant negative association between cardiovascular risk factors like BMI and CBF (Beason-Held et al., 2007; Dai et al., 2008; Jennings et al., 2013; Muller et al., 2012; Selim et al., 2008; Vernooij et al., 2008; Williamson et al., 2018). We found no significant association between grey matter perfusion and self-reported type 2 diabetes, number of cardiovascular conditions, hypercholesterolaemia, antihypertensive medication(s), CAGE score>2 or smoking, likely due to the small numbers of participants with these conditions in our study sample.

Accurate measurement of cerebral perfusion has proved challenging to date. Doppler ultrasound, like pCASL-MRI, is non-invasive, involves no exposure to exogenous contrast nor ionising radiation and is repeatable. However, it is highly operator dependent and estimation of flow within the vertebral arteries is particularly challenging. Additionally, measurements are limited to determination of arterial flow, which is a poor surrogate for tissue perfusion. [^{15}O]-water positron emission tomography (PET), like pCASL MRI, quantitatively measures total and region-specific CBF but is invasive, costly, complex, not widely available, requires injection of radioactive pharmaceuticals and exposure to ionising radiation and is therefore unsuitable for repeated studies. One of the main strengths of the present study is the use of pCASL-MRI to measure CBF. pCASL-MRI is a quantitative, non-invasive imaging technique, which does not employ ionising radiation nor exogenous contrast and which therefore potentially offers an acceptable method for population-based CBF assessment (Wintermark et al., 2005). Another strength of the present work is that robust estimates of the normal decline in CBF with age were possible due to the large sample size with a continuum of ages, and the robust statistical method (GAMLSS model) employed.

Although all pCASL-MRI examinations were performed using a state-of-the-art technique, guided by published recommendations, this technique is not without its limitations (Alsop et al., 2015). One such limitation is that the same labelling duration and delay were used in the acquisition of all participants' data, however, physiological inter-participant variations in cerebrovascular structure could impact these estimates and affect flow measurements, potentially leading to both under- and over-estimation of CBF. The PLD used in this study may have been too short to account for prolonged arterial transit times in older subjects, especially those with cerebrovascular disease. However, a PLD of 1800 ms was felt to be the optimal choice in our subject cohort amongst whom the mean age was less than 70 years. The ISMRM white paper recommends a slice thickness of 4-8 mm with no slice gap. In our study, we used a slice thickness of 8 mm and a 1 mm slice gap. Due to partial volume effects associated with thick slices, this may have resulted in underestimation of CBF (Alsaedi et al., 2018). The thick slices used in this study may also limit translatability of our results to other studies. Another potential issue with pCASL is imperfect labelling due to flow effects in the arteries, resulting in underestimation of CBF.

Although this study validates the notion that age and sex modify cerebral perfusion, the underlying mechanisms driving these changes cannot be determined in this cross-sectional study. Future waves of

Table 3

Normative values of pCASL-MRI cerebral perfusion stratified by age in male and female participants (n = 468).

	Age [years]						
Percentile	54	59	64	69	74	79	84
Male CBF$_{GM}$							
P95	51.6	50.3	49.1	47.8	46.5	45.2	43.9
P90	47.8	46.6	45.4	44.2	43.0	41.8	40.6
P75	42.1	41.1	40.0	39.0	37.9	36.9	35.8
P50	37.0	36.0	35.1	34.2	33.3	32.36	31.4
P25	32.1	31.3	30.5	29.7	28.9	28.11	27.3
P10	27.5	26.9	26.2	25.5	24.8	24.1	23.4
P05	24.8	24.2	23.5	22.9	22.3	21.7	21.1
Mean ± SD	37.6 ± 10.1	36.6 ± 9.9	35.7 ± 9.6	34.8 ± 9.4	33.8 ± 9.1	32.9 ± 8.9	31.9 ± 8.6
Female CBF$_{GM}$							
P95	56.3	55.1	53.8	52.5	51.2	49.9	48.6
P90	52.1	50.9	49.8	48.6	47.4	46.2	45.0
P75	46.0	44.9	43.9	42.8	41.8	40.7	39.7
P50	40.3	39.4	38.5	37.6	36.7	35.7	34.8
P25	35.1	34.3	33.5	32.7	31.9	31.1	30.3
P10	30.1	29.4	28.7	28.0	27.3	26.6	26.0
P05	27.0	26.4	25.8	25.2	24.6	24.0	23.3
Mean ± SD	41.0 ± 11.1	40.1 ± 10.8	39.1 ± 10.6	38.2 ± 10.3	37.3 ± 10.1	36.3 ± 9.8	35.4 ± 9.6

Age corresponds to exact year of age; values for intermediate ages should be estimated by interpolation between supplied values.

CBF$_{GM}$: whole grey matter cerebral blood flow [ml/100g/min]. SD = standard deviation.

TILDA MRI data collection will facilitate longitudinal investigation into the effects of age and sex on CBF.

5. Conclusion

This study is by far the largest single-site study to present normative reference values for CBF$_{GM}$ measured at 3T using pCASL-MRI in an aged community-dwelling cohort. These values will aid in the clinical interpretation of pCASL-MRI CBF$_{GM}$ measurements and in distinguishing age-related decline in CBF$_{GM}$ from pathological reduction. Given the significant effects of age and sex on CBF, these factors need to be taken into account when studying brain perfusion.

Ethics statement

All research was performed in accordance with the Declaration of Helsinki. Ethical approval was obtained for each wave of TILDA from the Health Sciences Research Ethics Committee at Trinity College Dublin, Dublin, Ireland, and all participants provided written informed consent. Those attending for MRI were required to complete an additional MRI-specific consent form and additional ethics approval was received from the St James's Hospital Research Ethic Committee, Dublin, Ireland.

Data for reference

The datasets generated during and/or analyzed during the current study are not publicly available due to data protection regulations but are accessible at TILDA on reasonable request. The procedures to gain access to TILDA data are specified at https://tilda.tcd.ie/data/accessing-data/. MRI analysis was performed using *Oxford_ASL* v4.0 in FMRIB Software Library (BASIL - FSL; Oxford Centre for Functional MRI of the Brain, Oxford, UK; https://fsl.fmrib.ox.ac.uk/fsl/fslwiki/BASIL) which is freely available to download here: https://github.com/ibme-qubic/oxasl.

Funding

CRediT author statement

Caoilfhionn Ní Leidhin: Conceptualization, Data curation, Formal analysis, Investigation, Methodology, Software, Validation, Visualization, Writing - original draft, Writing - review & editing Jason McMorrow: Data curation, Formal analysis, Investigation, Project administration, Resources, Software, Writing - review & editing Daniel Carey: Data curation, Formal analysis, Methodology, Validation, Writing - review & editing Louise Newman: Formal analysis, Methodology, Validation, Visualization, Writing - review & editing Wilby Williamson: Conceptualization, Methodology, Writing - review & editing Andrew J. Fagan: Data curation, Investigation, Methodology, Resources, Validation, Writing - review & editing Michael A. Chappell: Formal analysis, Methodology, Resources, Software, Validation, Writing - review & editing Rose Anne Kenny: Conceptualization, Funding acquisition, Investigation, Methodology, Project administration, Resources, Supervision, Writing - review & editing James F Meaney: Conceptualization, Funding acquisition, Investigation, Methodology, Project administration, Resources, Supervision, Writing - review & editing Silvin P. Knight: Conceptualization, Data curation, Formal analysis, Methodology, Project administration, Software, Supervision, Validation, Visualization, Roles/Writing - original draft, Writing - review & editing

Declaration of Competing Interest

None.

Acknowledgements

Supplementary materials

Supplementary material associated with this article can be found, in the online version, at doi:10.1016/j.neuroimage.2021.117741.

References

Alsaedi, A., Thomas, D., Bisdas, S., Golay, X., 2018. Overview and critical appraisal of arterial spin labelling technique in brain perfusion imaging. Contrast Media Mol. Imaging 2018, 5360375.

Alsop, D.C., Detre, J.A., Golay, X., Gunther, M., Hendrikse, J., Hernandez-Garcia, L., Lu, H., MacIntosh, B.J., Parkes, L.M., Smits, M., van Osch, M.J., Wang, D.J., Wong, E.C., Zaharchuk, G., 2015. Recommended implementation of arterial spin-labeled perfusion MRI for clinical applications: a consensus of the ISMRM perfusion study group and the European consortium for ASL in dementia. Magn. Reson. Med. 73, 102–116.

Beason-Held, L.L., Moghekar, A., Zonderman, A.B., Kraut, M.A., Resnick, S.M., 2007. Longitudinal changes in cerebral blood flow in the older hypertensive brain. Stroke 38, 1766–1773.

Buxton, R.B., 2005. Quantifying CBF with arterial spin labeling. J. Magn. Reson. Imaging 22, 723–726.

Chappell, M., MacIntosh, B., Okell, T., 2017. Introduction to Perfusion Quantification using Arterial Spin Labelling.

Chappell, M.A., Groves, A.R., Whitcher, B., Woolrich, M.W., 2009. Variational Bayesian inference for a nonlinear forward model. IEEE Trans. Signal Process. 57, 223–236.

Chen, J.J., Rosas, H.D., Salat, D.H., 2011. Age-associated reductions in cerebral blood flow are independent from regional atrophy. Neuroimage 55, 468–478.

Cronin, H., O'Regan, C., Finucane, C., Kearney, P., Kenny, R.A., 2013. Health and aging: development of the Irish Longitudinal Study on Ageing health assessment. J. Am. Geriatr. Soc. 61 (Suppl 2), S269–S278.

Dai, W., Lopez, O.L., Carmichael, O.T., Becker, J.T., Kuller, L.H., Gach, H.M., 2008. Abnormal regional cerebral blood flow in cognitively normal elderly subjects with hypertension. Stroke 39, 349–354.

de Roos, A., van der Grond, J., Mitchell, G., Westenberg, J., 2017. Magnetic resonance imaging of cardiovascular function and the brain: is dementia a cardiovascular-driven disease? Circulation 135, 2178–2195.

De Vis, J.B., Hendrikse, J., Bhogal, A., Adams, A., Kappelle, L.J., Petersen, E.T., 2015. Age-related changes in brain hemodynamics; a calibrated MRI study. Hum. Brain Mapp. 36, 3973–3987.

Dolui, S., Wang, Z., Wang, D.J.J., Mattay, R., Finkel, M., Elliott, M., Desiderio, L., Inglis, B., Mueller, B., Stafford, R.B., Launer, L.J., Jacobs Jr., D.R., Bryan, R.N., Detre, J.A., 2016. Comparison of non-invasive MRI measurements of cerebral blood flow in a large multisite cohort. J. Cereb. Blood Flow Metab. 36, 1244–1256.

Donoghue, O.A., McGarrigle, C.A., Foley, M., Fagan, A., Meaney, J., Kenny, R.A., 2018. Cohort profile update: The Irish Longitudinal Study on Ageing (TILDA). Int. J. Epidemiol. 47 1398-1398l.

Dorrance, A.M., Matin, N., Pires, P.W., 2014. The effects of obesity on the cerebral vasculature. Curr. Vasc. Pharmacol. 12, 462–472.

Fan, A.P., Jahanian, H., Holdsworth, S.J., Zaharchuk, G., 2016. Comparison of cerebral blood flow measurement with [15O]-water positron emission tomography and arterial spin labeling magnetic resonance imaging: a systematic review. J. Cereb. Blood Flow Metab..

Groves, A.R., Chappell, M.A., Woolrich, M.W., 2009. Combined spatial and non-spatial prior for inference on MRI time-series. Neuroimage 45, 795–809.

Haller, S., Zaharchuk, G., Thomas, D.L., Lovblad, K.O., Barkhof, F., Golay, X., 2016. Arterial spin labeling perfusion of the brain: emerging clinical applications. Radiology 281, 337–356.

Jefferson, A.L., Cambronero, F.E., Liu, D., Moore, E.E., Neal, J.E., Terry, J.G., Nair, S., Pechman, K.R., Rane, S., Davis, L.T., Gifford, K.A., Hohman, T.J., Bell, S.P., Wang, T.J., Beckman, J.A., Carr, J.J., 2018. Higher aortic stiffness is related to lower cerebral blood flow and preserved cerebrovascular reactivity in older adults. Circulation 138, 1951–1962.

Jennings, J.R., Heim, A.F., Kuan, D.C., Gianaros, P.J., Muldoon, M.F., Manuck, S.B., 2013. Use of total cerebral blood flow as an imaging biomarker of known cardiovascular risks. Stroke 44, 2480–2485.

Juttukonda, M.R., Donahue, M.J., 2019. Neuroimaging of vascular reserve in patients with cerebrovascular diseases. Neuroimage 187, 192–208.

Kearney, P.M., Cronin, H., O'Regan, C., Kamiya, Y., Savva, G.M., Whelan, B., Kenny, R., 2011. Cohort profile: the Irish Longitudinal Study on Ageing. Int. J. Epidemiol. 40, 877–884.

Kenny, R.A., Coen, R.F., Frewen, J., Donoghue, O.A., Cronin, H., Savva, G.M., 2013. Normative values of cognitive and physical function in older adults: findings from the Irish Longitudinal Study on Ageing. J. Am. Geriatr. Soc. 61 (Suppl 2), S279–S290.

Lee, C., Lopez, O.L., Becker, J.T., Raji, C., Dai, W., Kuller, L.H., Gach, H.M., 2009. Imaging cerebral blood flow in the cognitively normal aging brain with arterial spin labeling: implications for imaging of neurodegenerative disease. J. Neuroimaging 19, 344–352.

Leijenaar, J.F., van Maurik, I.S., Kuijer, J.P.A., van der Flier, W.M., Scheltens, P., Barkhof, F., Prins, N.D., 2017. Lower cerebral blood flow in subjects with Alzheimer's dementia, mild cognitive impairment, and subjective cognitive decline using two-dimensional phase-contrast magnetic resonance imaging. Alzheimers Dement. 9, 76–83.

Liu, Y., Zhu, X., Feinberg, D., Guenther, M., Gregori, J., Weiner, M.W., Schuff, N., 2012. Arterial spin labeling MRI study of age and gender effects on brain perfusion hemodynamics. Magn. Reson. Med. 68, 912–922.

Lu, H., Xu, F., Rodrigue, K.M., Kennedy, K.M., Cheng, Y., Flicker, B., Hebrank, A.C., Uh, J., Park, D.C., 2011. Alterations in cerebral metabolic rate and blood supply across the adult lifespan. Cereb. Cortex 21, 1426–1434.

Luckhaus, C., Fluss, M.O., Wittsack, H.J., Grass-Kapanke, B., Janner, M., Khalili-Amiri, R., Friedrich, W., Supprian, T., Gaebel, W., Modder, U., Cohnen, M., 2008. Detection of changed regional cerebral blood flow in mild cognitive impairment and early Alzheimer's dementia by perfusion-weighted magnetic resonance imaging. Neuroimage 40, 495–503.

Muller, M., van der Graaf, Y., Visseren, F.L., Mali, W.P., Geerlings, M.I., Group, S.S., 2012. Hypertension and longitudinal changes in cerebral blood flow: the SMART-MR study. Ann. Neurol. 71, 825–833.

Ogg, R.J., Kingsley, P.B., Taylor, J.S., 1994. WET, a T1- and B1-insensitive water-suppression method for in vivo localized 1H NMR spectroscopy. J. Magn. Reson. B 104, 1–10.

Parkes, L.M., Rashid, W., Chard, D.T., Tofts, P.S., 2004. Normal cerebral perfusion measurements using arterial spin labeling: reproducibility, stability, and age and gender effects. Magn. Reson. Med. 51, 736–743.

Pires, P.W., Dams Ramos, C.M., Matin, N., Dorrance, A.M., 2013. The effects of hypertension on the cerebral circulation. Am. J. Physiol. Heart Circ. Physiol. 304, H1598–H1614.

Preibisch, C., Sorg, C., Forschler, A., Grimmer, T., Sax, I., Wohlschlager, A.M., Perneczky, R., Forstl, H., Kurz, A., Zimmer, C., Alexopoulos, P., 2011. Age-related cerebral perfusion changes in the parietal and temporal lobes measured by pulsed arterial spin labeling. J. Magn. Reson. Imaging 34, 1295–1302.

Rigby, R., Stasinopoulos, D., 2005. Generalized additive models for location, scale and shape. J. R. Stat. Soc. 54, 507–554.

Rigby, R.A., Stasinopoulos, D.M., 2004. Smooth centile curves for skew and kurtotic data modelled using the Box-Cox power exponential distribution. Stat. Med. 23, 3053–3076.

Rogers, R.L., Meyer, J.S., Mortel, K.F., Mahurin, R.K., Thornby, J., 1985. Age-related reductions in cerebral vasomotor reactivity and the law of initial value: a 4-year prospective longitudinal study. J. Cereb. Blood Flow Metab. 5, 79–85.

Selim, M., Jones, R., Novak, P., Zhao, P., Novak, V., 2008. The effects of body mass index on cerebral blood flow velocity. Clin. Auton. Res. 18, 331–338.

Soni, N., Jain, A., Kumar, S., Pandey, C.M., Awasthi, A., 2016. Arterial spin labeling magnetic resonance perfusion study to evaluate the effects of age and gender on normal cerebral blood flow. Neurol. India 64, S32–S38 Suppl.

Tarumi, T., Zhang, R., 2018. Cerebral blood flow in normal aging adults: cardiovascular determinants, clinical implications, and aerobic fitness. J. Neurochem. 144, 595–608.

Thomas, B., Sheelakumari, R., Kannath, S., Sarma, S., Menon, R.N., 2019. Regional cerebral blood flow in the posterior cingulate and precuneus and the entorhinal cortical atrophy score differentiate mild cognitive impairment and dementia due to Alzheimer disease. AJNR Am. J. Neuroradiol. 40, 1658–1664.

United Nations, 2015. Population Division D.o.E.a.S.A.. World Population Ageing.

Vernooij, M.W., van der Lugt, A., Ikram, M.A., Wielopolski, P.A., Vrooman, H.A., Hofman, A., Krestin, G.P., Breteler, M.M., 2008. Total cerebral blood flow and total brain perfusion in the general population: the Rotterdam Scan Study. J. Cereb. Blood Flow Metab. 28, 412–419.

Whelan, B.J., Savva, G.M., 2013. Design and methodology of the Irish Longitudinal Study on Ageing. J. Am. Geriatr. Soc. 61 (Suppl 2), S265–S268.

Williamson, W., Lewandowski, A.J., Forkert, N.D., Griffanti, L., Okell, T.W., Betts, J., Boardman, H., Siepmann, T., McKean, D., Huckstep, O., Francis, J.M., Neubauer, S., Phellan, R., Jenkinson, M., Doherty, A., Dawes, H., Frangou, E., Malamateniou, C., Foster, C., Leeson, P., 2018. Association of cardiovascular risk factors with MRI indices of cerebrovascular structure and function and white matter hyperintensities in young adults. JAMA 320, 665–673.

Willie, C.K., Tzeng, Y.C., Fisher, J.A., Ainslie, P.N., 2014. Integrative regulation of human brain blood flow. J. Physiol. 592, 841–859.

Wintermark, M., Sesay, M., Barbier, E., Borbely, K., Dillon, W.P., Eastwood, J.D., Glenn, T.C., Grandin, C.B., Pedraza, S., Soustiel, J.F., Nariai, T., Zaharchuk, G., Caille, J.M., Dousset, V., Yonas, H., 2005. Comparative overview of brain perfusion imaging techniques. J. Neuroradiol. 32, 294–314.

Wolters, F.J., Zonneveld, H.I., Hofman, A., van der Lugt, A., Koudstaal, P.J., Vernooij, M.W., Ikram, M.A.Heart-Brain Connection Collaborative Research, G., 2017. Cerebral perfusion and the risk of dementia: a population-based study. Circulation 136, 719–728.

Woolrich, M.W., Jbabdi, S., Patenaude, B., Chappell, M., Makni, S., Behrens, T., Beckmann, C., Jenkinson, M., Smith, S.M., 2009. Bayesian analysis of neuroimaging data in FSL. Neuroimage 45, S173–S186.

World Health Organization, 2015. World Report on Ageing and Health. World Health Organization.

Zhang, N., Gordon, M.L., Goldberg, T.E., 2017. Cerebral blood flow measured by arterial spin labeling MRI at resting state in normal aging and Alzheimer's disease. Neurosci. Biobehav. Rev. 72, 168–175.

Zhang, N., Gordon, M.L., Ma, Y., Chi, B., Gomar, J.J., Peng, S., Kingsley, P.B., Eidelberg, D., Goldberg, T.E., 2018. The age-related perfusion pattern measured with arterial spin labeling MRI in healthy subjects. Front. Aging Neurosci. 10, 214.

Zonneveld, H.I., Loehrer, E.A., Hofman, A., Niessen, W.J., van der Lugt, A., Krestin, G.P., Ikram, M.A., Vernooij, M.W., 2015. The bidirectional association between reduced cerebral blood flow and brain atrophy in the general population. J. Cereb. Blood Flow Metab. 35, 1882–1887.